Biochimica et Biophysica Acta, 934 (1988) 235–246
Elsevier

BBA 42795

Surface-enhanced Raman scattering spectroscopy: probing the lumenal surface of Photosystem II membranes for evidence of manganese

Michael Seibert [a,c], Therese M. Cotton [b] and James G. Metz [c,*]

[a] *Department of Biological Sciences, University of Denver, CO,* [b] *Department of Chemistry, University of Nebraska, Lincoln, NE and* [c] *Photoconversion Research Branch, Solar Energy Research Institute* **, *Golden, CO (U.S.A.)*

(Received 29 December 1987)

Key words: Oxygen evolution; Manganese; Photosynthesis; Spectroscopy; Photosystem II; Chloride; Bromide; Surface enhanced Raman scattering spectroscopy

A surface-enhanced Raman scattering (SERS) peak at 225 cm^{-1} was reported in detergent-extracted, O_2-evolving Photosystem II (PS II) appressed membrane fragments from spinach that were treated with $CaCl_2$ (Seibert, M. and Cotton, T. (1985) FEBS Lett. 182, 34–38). $CaCl_2$ removes the 17-, 23-, and 33-kDa extrinsic proteins associated with O_2 evolution from the surface of the membrane without extracting functional Mn. The same peak has now been observed in PS II-enriched membrane fragments from *Scenedesmus obliquus*. The signal is related to the presence of Mn in spinach PS II membranes but not to the presence of Ca, Mg or Fe. Substitution of Br^- for Cl^- in the membranes without displacing Mn shifts the peak from 225 cm^{-1} to 140 cm^{-1}. However, this shift is too great for the source of the SERS signals to be explained by simple Mn-Cl or Mn-Br vibrational modes. Evidence in addition to that presented in the previous publication indicates that the 33-kDa protein covers that part of the membrane that is the cause of the SERS signal. Due to altered properties of the SERS signal in the LF-1 mutant of *Scenedesmus*, which is affected in the D1 protein and binds less Mn than the wild type, we suggest that the 33-kDa protein shields a Mn-binding site on the D1 protein. Possible sources of the signal include (1) an Mn-O or Mn-N vibrational mode modified by chloride not present in the first coordination sphere; (2) a cooperative effect associated with the protein environment around the Mn-binding site that changes with the presence of halide; or (3) a species associated primarily with the Ag electrode surface that changes depending on the presence or absence of Mn and halide on the membrane surface. This last possibility might explain some of the results obtained with Br-treated spinach and Ca-treated *Scenedesmus* LF-1 mutant membranes.

---

* Current address: CR&D, E-402, Experimental Station, E.I. DuPont Comp., Wilmington, DE 19898, U.S.A.

** Operated by the Midwest Research Institute for the U.S. Department of Energy under contract DE-AC-02-83CH10093.

Abbreviations: DCBQ, 2,6-dichlorobenzoquinone; DMBQ, 2,6-dimethylbenzoquinone; EPR, electron paramagnetic resonance; EXAFS, extended X-ray absorption fine structure; LDS-PAGE, lithium dodecyl sulfate polyacrylamide gel electrophoresis; Mes, 4-morpholineethanesulfonic acid; OEC, oxygen-evolving complex; OES II, oxygen-evolving Photosystem II; PS, Photosystem I; PS II, Photosystem II; SCE, standard calomel electrode; SERS, surface-enhanced Raman scattering; SERRS, surface-enhanced resonance Raman scattering; S_n, $n = 0–4$, S-state; WT, wild-type.

Correspondence: M. Seibert, Photoconversion Research Branch, Solar Energy Research Institute, Golden, CO 80401, U.S.A.

Introduction

Considerable progress has been made over the past 10 years in the development of surface-enhanced Raman scattering (SERS) spectroscopy as a technique and in the understanding of the enhancement phenomenon on a theoretical basis [1]. Enhancement in Raman or resonance Raman scattering results when molecules are adsorbed onto or near the surface of certain metals, including silver, gold and copper. The effect was first observed for pyridine adsorbed onto roughened silver electrodes [2–4], where an enhancement of 10^6 over the normal Raman scattering intensity was determined [3,4]. The magnitude of the enhancement is dependent upon several variables, including the nature of the metal substrate, the roughness of the surface, the adsorbate, and the electrochemical potential imposed on the sample.

Theoretical explanations for the enhancement process can be divided into two major categories – chemical and electromagnetic [5–7]. The former proposes that chemical interactions between the adsorbate and the metal leads to profound changes in the molecular polarizability of the adsorbed molecule, which, in turn, results in enhanced Raman scattering. The latter is based upon classical electromagnetic theory, which predicts an enhancement of the electromagnetic field due to incident and Raman scattered light near metal particle surfaces. At present, most theorists agree that both types of effects are important in the SERS process.

Many different small molecules have been studied on SERS-active metals [8]. However, the use of SERS or, moreover, surface-enhanced resonance Raman scattering (SERRS) for the study of complex biomolecules, has been limited. SERS spectra from amino acids and proteins [9]; nucleic acids, polynucleotides, and DNA [10–13]; and lipid monolayers [14] have been reported. SERRS occurs when the wavelength of laser excitation is in resonance with an electronic transition in the adsorbate. The magnitude of the enhancement is dependent upon the absorption coefficient of the adsorbate and the structure of the metal surface. A number of SERRS studies have been performed on proteins or protein complexes that contain chromophores. These include heme proteins [15,16], glucose oxidase [17,18] and bacterial reaction centers [19].

We have recently reported the application of SERS and SERRS techniques to biological membrane systems [20,21]. Detergent-fractionated Photosystem II (PS II)-enriched membranes which evolve O_2 (OES II membranes), were chosen for the initial studies [20] because (1) they have been used extensively in recent attempts to further understand the process of photosynthetic water oxidation; (2) they contain a number of chromophores easily detectable by SERRS; and (3) the geometry of the membrane system was ideally suited for the technique. In explanation of this last point, OES II membranes are isolated appressed membrane fragments from grana thylakoids [22]. Structurally, they are double membranes, geometrically symmetric about a plane between the two membrane sheets; and the water-splitting enzyme complex is located on both external surfaces (the lumenal surface of the intact grana thylakoid) of the membrane 'sandwich' [22]. Consequently, it

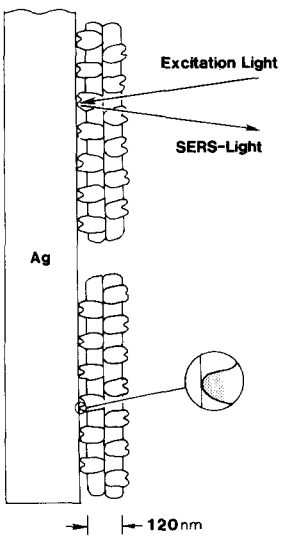

Fig. 1. An expanded view of an Ag, SERS-sensitive electrode. Isolated PS II membranes are adsorbed onto the surface of the silver. Note that the geometry of membranes is such that it does not matter which surface of the appressed membrane 'sandwich' is adsorbed onto the silver. Both surfaces are equivalent as discussed in the text. Laser light coming from the right is back-scattered by the sample membrane. Light scattered by that part of the membrane lying closest to the silver surface (roughly, the shaded area of the expanded inset) is subjected to the enhanced Raman scattering effect described in the text.

does not matter which surface is adsorbed onto the SERS-active metal (Fig. 1). In either case the surface properties of the membrane are the same, and hence any SERS spectrum obtained would be the same. This particular membrane geometry eliminates the possibility that the results obtained are a mixture of properties associated with both sides of the same membrane.

The purpose of the present study is to characterize a 225 cm^{-1} SERS signal that we discovered in spinach OES II membranes from which three extrinsic proteins associated with photosynthetic O_2-evolution were removed by $CaCl_2$ treatment [20]. This treatment does not significantly affect the Mn content of the membrane [23]. Many questions that one can raise about this new SERS signal are as yet unanswered. For example, can it be observed in species other than spinach? Since it seems to be related to membrane-bound Mn and O_2 evolution [20], is it a direct or indirect probe for Mn and thus O_2 evolution competency? What is the chemical nature of the vibrational mode that gives rise to the signal? Finally, can this new probe serve to help clarify our understanding of the water-oxidation process of photosynthesis? These and other questions will be addressed.

Materials and Methods

Biological samples. OES II membranes from market spinach were isolated by the K & M procedure using Triton X-100; the preparation is essentially free of Photosystem I (PS I) pigment contamination [22]. Note that this time we used a Triton/Chl ratio of 25 : 1 (w/w). The ratio may have to be adjusted slightly at different times of the year to maximize recovery yield and minimize PS I contamination. Steady-state O_2-evolution rates were assayed with a Clark electrode and a heat-filtered incandescent light source using the indicated acceptors in a buffer containing 20 mM Mes (pH 6.0), 15 mM NaCl (or NaBr where indicated), and 300 mM sucrose. Rates of 313 μmol O_2 per mg Chl per h were obtained using 2 mM 2,6-dimethylbenzoquinone (DMBQ) as an acceptor and 666 μmol O_2 per mg Chl per h using 0.4 mM 2,6-dichlorobenzoquinone (DCBQ) as an acceptor. Ogilvie et al. [24] and more recently Ikeuchi et al. [25] have shown that the rate of O_2 evolution in OES II membranes depends on the acceptor used.

PS II-enriched membranes from wild type (WT) and LF-1 mutant cells of *Scenedesmus obliquus* were obtained using the procedure of Metz and Seibert [26]. Although these membrane preparations contain some PS I pigments, they appear to be structurally similar to the higher plant PS II membranes because (1) they can be pelleted by centrifugation under similar conditions and (2) $CaCl_2$ treatment releases three extrinsic proteins associated with O_2 evolution into the suspending medium. O_2 evolution rates for the WT preparations were between 150 and 200 μmol per mg Chl per h using DCBQ as an acceptor. The mutant, of course, does not evolve O_2 [27].

Sample treatments. The three extrinsic proteins (17, 23 and 33 kDa), located on the lumenal surface of PS II-enriched membranes and associated with the O_2-evolution process, were removed from the membranes by the procedure of Ono and Inoue [23], except that 0.8 or 0.9 M $CaCl_2$ was used instead of 1.0 M. For the $MgCl_2$ treatments, 0.8 M was used instead of 1.0 M [23]. As mentioned before, this treatment does not remove functional Mn from the membrane. After $CaCl_2$ treatment (1 mg Chl/ml) at 4 °C for 30 min in the dark, the samples were washed twice in 40 mM Mes (pH 6.5), 200 mM NaCl, and 300 mM sorbitol by centrifugation (30 000 × g for 10 min to remove Ca^{2+} and lower the Cl^- concentration); resuspended in 20 mM Mes (pH 6.5), 5 mM $MgCl_2$, 15 mM NaCl, and 400 mM sucrose at 3.6 mg Chl/ml; and stored for less than 2 weeks in small vials at −80 °C until use.

$CaBr_2$ treatments were performed in a similar manner. Spinach OES II membranes were washed twice in 40 mM Mes (pH 6.5) and 300 mM sorbitol; resuspended in 40 mM Mes (pH 6.5), 10 mM NaBr, 300 mM sorbitol, and then treated with the indicated amount of $CaBr_2$ in the same buffer for 30 min in the dark at 4 °C. The final Chl concentration during treatment was 1 mg/ml. After pelleting, the samples were washed twice in 40 mM Mes (pH 6.5), 150 mM NaBr, and 300 mM sorbitol and stored at about 2.5 mg/ml Chl in 20 mM Mes, 15 mM NaBr, and 400 mM sucrose at −80 °C in small vials until use. For SERS studies the 0.2 M $CaBr_2$-treated samples

were stored in 5 mM $MgBr_2$ in addition to the above-mentioned storage buffer.

LDS-PAGE using a 10–15% acrylamide gradient was described previously [26]. Samples were solubilized in 10 mM Tricine (pH 7.8), 10% (w/v) sucrose, and 1% LDS at 65°C for 4 min. Subsequently, 30 mM dithiothreitol was added at room temperature prior to electrophoresis at 5°C. Samples were loaded on an equal chlorophyll basis (12 μg per lane). Molecular mass standards were from Bio-Rad Laboratories (Richmond, CA).

Heat treatment of $CaCl_2$-extracted membranes was accomplished by exposing the samples in a glass test tube to a 53°C water bath for 5 min. Iron and manganese analyses were performed using a Perkin-Elmer No. 2380 Atomic Absorption Spectrometer with a graphite furnace. The final values were corrected for the amount of Fe or Mn contamination in the sample buffer.

SERS equipment and techniques. Surface-enhanced Raman spectra were recorded using the 514.5 nm line (30 mW) of an argon ion laser (INNOVA 90-5, Coherent Inc., Palo Alto, CA) as an excitation source. The spectrometer geometry is shown in Fig. 2. Raman scattered light from the sample cuvette (see Fig. 1 for an expanded view of the Ag working electrode) was collected in the backscattering mode and focused through a Canon 55 mm, *f*/1.2 camera lens onto the slits of the monochromator. A Spex 1877 Triplemate monochromator/spectrograph, equipped with a 1200 grooves/mm grating with a slit width of 0.200 nm in the spectrograph stage, was used to disperse the light across the detector. The detector, an intensified silicon photodiode array (PAR 1420), was maintained at −20°C. Spectra were acquired and manipulated using OMA II (PAR 1215 console and 1218 controller) software. Single scans were collected using 60 delays (approx. 1 s integration time); multiple scans, when employed, are indicated in the figure legends.

The electrochemical cell (sample cuvette in Fig. 2) used in these experiments has been described [21,28]. Electrolyte, consisting of 20 mM Mes (pH 6.0), 100 mM Na_2SO_4, and 300 mM sucrose in deionized/distilled water, was degassed by N_2 purging prior to addition of the biological samples (6 μg Chl/ml) and subsequent anodization of the Ag electrode. Care was taken to minimize the Cl^-

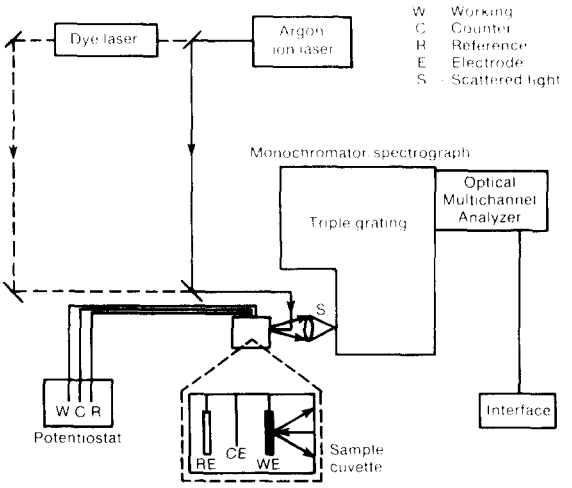

Fig. 2. Surface-enhanced Raman scattering spectrometer. Light from an argon ion laser is focused on a SERS-active Ag electrode located in the sample cuvette or electrochemical cell. The Ag working electrode (WE), a Ag/AgCl reference electrode (RE), and a platinum counter electrode (CE) are all connected to a potentiostat. The cuvette contained 15 ml of buffer (100 mM Na_2SO_4, 300 mM sucrose, and 20 mM Mes (pH 6.0)) and the OES II sample membranes. Light scattered from the interface between the surface of the Ag electrode and the adsorbed membranes (see Fig. 1 for an expanded view) is collected by a lens (S) and focused onto the input slits of a triplet monochromator. The output is detected by an optical multichannel analyzer.

concentration in the biological samples, since Cl^- interactions with the Ag electrode can result in SERS artifacts that have spectra similar to the SERS signals reported in this study. The Ag electrode was prepared from flattened polycrystalline Ag wire (Goldsmith, Evanston, IL) and sealed into a glass holder using Torr Seal (Varian Assoc., Palo Alto, CA). The anodization procedure serves two purposes. First, it provides a clean surface by removing any oxide layer or adsorbed impurities from the electrode surface. Second, the surface is roughened following the redeposition of Ag. The surface roughness provides an enhancement factor of approx. 3–4 orders of magnitude. The anodization process itself consisted of stepping the electrode from −0.2 V vs. SCE (all potentials will be referenced to SCE hereafter) to +0.45 V and allowing 25 mCi/cm^2 charge to pass, followed by stepping the electrode back to −0.2 V. During all experiments reported below, the electrode potential was maintained at −0.2 V, since control ex-

periments indicated that maximum signal intensity occurred at this potential. The experiments in Figs. 5 and 10 were accomplished by monitoring the SERS signals at the indicated times. The electrode was maintained at −0.2 V in the above-mentioned electrolyte at room temperature and kept in the dark between monitoring scans to avoid unnecessary photodegradation of the biological material.

Results

SERS spectra

In a previous paper, we reported a low frequency SERS signal at 225 cm^{-1} in $CaCl_2$-treated spinach OES II membranes [20]. Fig. 3 shows that the 225 cm^{-1} signal is not observed in control OES II membranes but appears when three extrinsic proteins associated with photosynthetic O_2 evolution are removed from the surface of the membrane. The three proteins are located physically on the top of 8 nm high protrusions which rise from the surface of the membrane sheet [29]. Both $CaCl_2$ and $MgCl_2$ remove these proteins without removing functional Mn (Ref. 23; see also Table I later in this paper), and both unmask the same SERS signal. This experiment indicates that the vibrational mode giving rise to the 225 cm^{-1} band is not associated with Ca or Mg per se, since

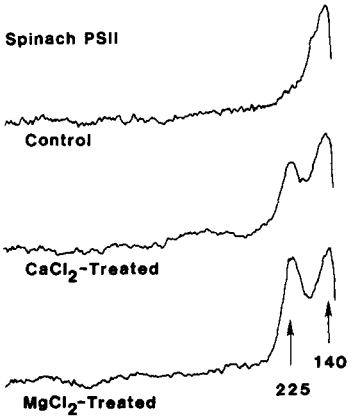

Fig. 3. Low-frequency SERS spectra of spinach OES II membranes. Control membranes do not display a peak at 225 cm^{-1}. However, treatment of OES II membranes with 0.9 M $CaCl_2$ or 0.8 M $MgCl_2$ unmasks a SERS signal at 225 cm^{-1}. A second peak at about 140 cm^{-1} is not affected by any of the treatments. Chl, 6 μg/ml. Temperature, 22° C. Scans, 16.

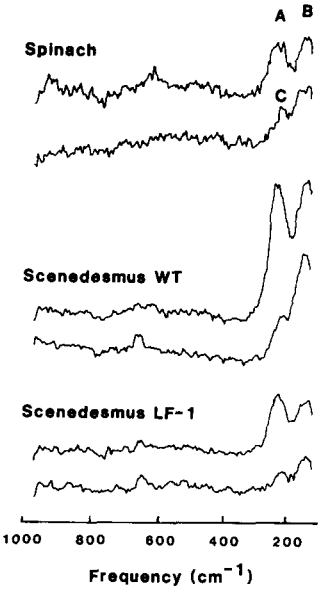

Fig. 4. Low-frequency SERS spectra of OES II membranes subjected to $CaCl_2$ treatment. Spectra of spinach, *Scenedesmus* WT, and *Scenedesmus* LF-1 mutant membranes are compared either with those of a buffer blank (spinach) or with membranes aged in the sample cuvette to the point that their Raman scattering properties no longer change (WT and LF-1). Peaks A and B refer to spectra of fresh membrane samples and shoulder C refers to the spectra of the blank control or aged membranes. The spinach data were obtained in a single scan while the data for WT and LF-1 were an average of 16 scans. The frequency range of the SERS peaks were as follows: A: 222–225 cm^{-1}, B: 128–153 cm^{-1}, and C: 209–213 cm^{-1}. Chl, 6 μg/ml. Temperature, 21° C.

the peak frequency is independent of the cation used. These spectra show features further into the low frequency region than did our previous study [20]. However, the peak at 140 cm^{-1} is not affected by any of the treatments. Fig. 4 demonstrates that a similar SERS signal (peak A) can also be seen in $CaCl_2$-treated PS II membranes isolated from *Scenedesmus* WT and LF-1 thylakoids. Signal averaging does not influence the general features of the spectra. Note that the peak in the 130–150 cm^{-1} range * (peak B) appears to be the same in the sample and the background spectra. It is probably due to Ag_4^+ clusters on the

* Our detector is not well calibrated below 200 cm^{-1}, so we do not place much significance on apparent differences in peak maxima in the 130–150 cm^{-1} range.

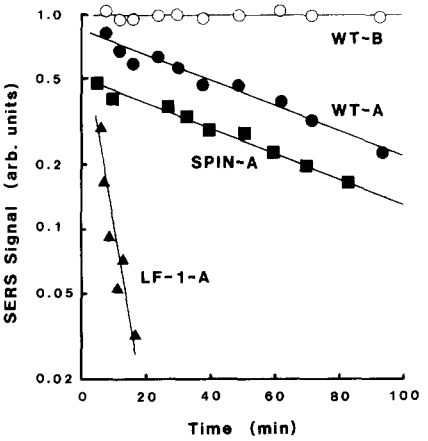

Fig. 5. Decay kinetics of peak A for spinach (SPIN), *Scenedesmus* WT (WT), and *Scenedesmus* LF-1 (LF-1) OES II membranes and peak B for *Scenedesmus* WT PS II membranes. Samples and conditions were the same as those in Fig. 4, except that data were taken at the indicated times (see Materials and Methods). Scans, 16.

Ag electrode [30] and is not a property of the membrane. The small peak at about 210 cm^{-1} (peak C) in the background spectra is due to Ag-O [31] or less likely to Ag-Cl [32] vibrations, again a property of the Ag electrode surface. Fig. 5 shows the dark decay kinetics of both peaks A and B of Fig. 4 under the conditions present at the surface of the Ag electrode. Peak A decreases with time in both spinach and *Scenedesmus* membranes, while peak B is stable (only *Scenedesmus* WT data is shown in Fig. 5). The half-time for the disappearance of peak A in $CaCl_2$-treated spinach and WT algal PS II membranes is about 48 min. That in the *Scenedesmus* LF-1 mutant membranes is much shorter, about 3 min.

Mn and Fe content of OES II membranes

Fig. 6 shows the relationship between O_2-evolving capacity and Mn content in $CaCl_2$-treated OES II membranes. Light-induced O_2-evolution capacity was demonstrated by including 50 mM $CaCl_2$ in the O_2 assay medium as originally demonstrated by Ono and Inoue [33]. The disappearance of peak A in $CaCl_2$-treated spinach OES II membranes (Fig. 5) has been correlated kinetically with the loss of O_2-evolving capacity in the preparation and also has been related to the release of Mn from the membrane by Tris treatment

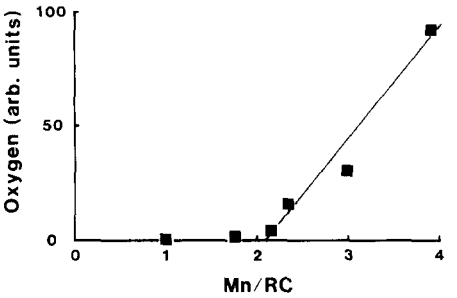

Fig. 6. Relationship between the amount of O_2-evolving capacity and the amount of Mn in 0.9 M $CaCl_2$-treated OES II membranes from spinach. Samples were assayed for O_2 in the presence of 50 mM $CaCl_2$ (100 = 61 μmol O_2 per mg Chl per h). Different amounts of Mn per reaction center (RC) were obtained by allowing the samples to age in low salt buffer (15 mM NaCl) at 4 °C in the dark for various periods of time (up to 36 h). A Chl-to-RC ratio of 220 : 1 was used.

[20]. Fig. 7 shows that the peak also disappears immediately upon heat treatment or H_2O_2 treatment of $CaCl_2$-treated OES II membranes. Heat treatment and H_2O_2 treatment plus light [34] are known to release Mn from Ca-treated OES II membranes. All these data suggest a direct correlation between the 225 cm^{-1} SERS signal observed in OES II membranes stripped of the three extrinsic proteins and the presence of functional

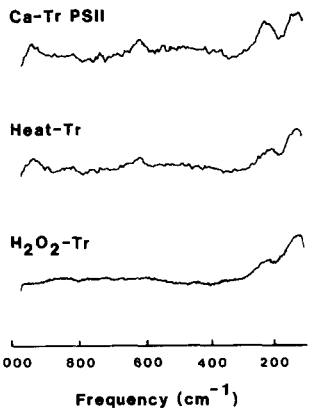

Fig. 7. SERS spectra of fresh $CaCl_2$-treated OES II membranes from spinach and a similar sample a few minutes later right after heat treatment at 53 °C for 5 min. For comparison a spectrum of fresh $CaCl_2$-treated OES II to which 6 mM H_2O_2 was added directly into the sample cuvette is also shown. Heat and H_2O_2 treatments remove most of the functional Mn from the PS II membranes. The peak frequencies are 223 and 138 cm^{-1} (control) and 213 and 139 cm^{-1} (treated). The spectra are an average of 5 or 16 (H_2O_2-Tr) scans.

TABLE I

MANGANESE AND IRON ANALYSES OF OES II MEMBRANES

Sample	Mn per 220 Chl	Mn per 400 Chl [a]	Fe per 220 Chl
Spinach			
Control OES II membranes	3.7	–	4.3
$CaCl_2$-treated OES II membranes	3.9	–	3.8
Tris-treated OES II membranes [b]	0.5	–	4.8
Scenedesmus PS II membranes			
$CaCl_2$-treated WT	–	3.8	–
$CaCl_2$-treated LF-1	–	2.2	–

[a] PS II-enriched membranes from *Scenedesmus* contain PS I pigment contamination and at least 20% of the PS II reaction centers are inactive, thus the high estimate of 400 Chl per active PS II reaction center compared to 220 in highly purified spinach OES II.
[b] Treated with 0.8 M Tris HCl (pH 9.3) for 30 min in room light at 4°C. Tris and solubilized Mn were removed by centrifugation.

Mn (i.e., that involved in the photosynthetic water-splitting process) in the membranes. Although we have suggested that the 225 cm^{-1} signal might be related to an Mn-ligand vibration, we were unable to ascertain the exact origin of the signal [20]. Besides the possibility that Mn-Cl, Mn-N, or Mn-O vibrational modes were being detected, it was equally likely that Fe-ligand vibrations were being observed. Iron is present in PS II, and Fe-N resonance Raman peaks have also been reported at about 220 cm^{-1} [35]. In Table I we show Mn and Fe analyses of PS II membranes subjected to $CaCl_2$ and Tris treatments. Calcium treatment does not release functional Mn, but Tris treatment releases nearly 90% of the membrane-bound Mn. Neither treatment greatly affects iron content, though the amount of iron in the material from sample-to-sample is variable (data not shown). These data eliminate the possibility that the 225 cm^{-1} signal is related to iron. Table I also shows comparative figures for the amount of Mn found in $CaCl_2$-treated *Scenedesmus* WT and LF-1 PS II-enriched membranes. The mutant contains 58% of the Mn found in WT membranes.

Bromide substitution for chloride

In order to further ascertain the character of a putative Mn-ligand vibration contributing to the 225 cm^{-1} SERS peak, we substituted bromide for chloride in spinach OES II membranes. To do this, it was necessary both to execute the halide substitution and to remove the three extrinsic proteins. Fig. 8 is an LDS gel showing the results

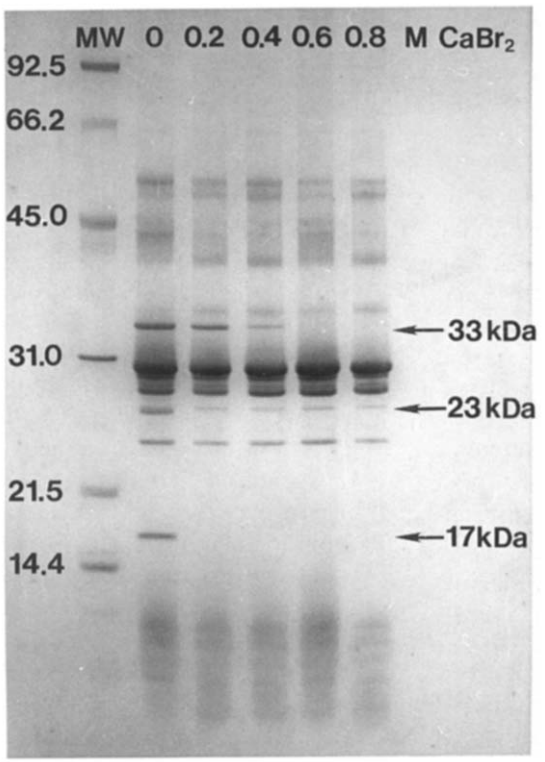

Fig. 8. LDS-PAGE of spinach OES II membranes exposed to the indicated concentrations of $CaBr_2$. Treatment with 0.2 M $CaBr_2$ removes the 17- and 23-kDa extrinsic proteins associated with water-oxidation function while 0.6 M is sufficient to remove the 33-kDa extrinsic protein, in addition. The lightly staining band right above the 33-kDa protein is the D1 (Q_B) protein [36] which functions on the oxidizing side of the PS II reaction center [26,27,36] and is a component of isolated PS II reaction center complexes [37,38]. MW indicates molecular-weight standards.

TABLE II

EFFECT OF CALCIUM TREATMENT ON SPINACH OES II MEMBRANES

Values in parentheses are the ratios of O_2 evolution in the presence and absence of $CaBr_2$ or $CaCl_2$ added to the O_2 assay medium.

Treatment		O_2 (μmol per mg Chl per h)	O_2 (μmol per mg Chl per h) 50 mM $CaBr_2$, included in assay	O_2 (μmol per mg Chl per h) 50 mM $CaCl_2$, included in assay
$CaBr_2$ *	0.0 M	313	–	–
	0.2 M	98	199 (2.0)	–
	0.4 M	23	95 (4.1)	–
	0.6 M	8	58 *** (7.2)	–
	0.8 M	5	23 (4.6)	–
$CaCl_2$ **	0.7 M	25	–	59 (2.4)
	0.8 M	8	–	39 *** (4.9)
	0.9 M	12	–	43 (3.6)

* Assay medium: 1 mM DMBQ in 20 mM Mes (pH 6.0), 10 mM NaBr, 300 mM sucrose.

** Assay medium: 1 mM DMBQ in 20 mM Mes (pH 6.0), 10 mM NaCl, 300 mM sucrose.

*** O_2-evolution rates obtained by this assay for OES II membranes which lack the three extrinsic proteins but which contain about four Mn per PS II reaction center are about 20% of those observed in control OES II membranes which bind the three extrinsic proteins (Ref. 33, Table I, Fig. 6).

of washing Br-substituted OES II membranes with increasing amounts of $CaBr_2$. As can be seen, $CaBr_2$ removes the extrinsic proteins at least as efficiently as the $CaCl_2$-washing procedure described by Ono and Inoue [23]. Treatment with 0.2 M $CaBr_2$ removed the 17- and 23-kDa proteins while 0.6 M was sufficient to remove all three proteins. Note that the calcium-treated samples were washed in a buffer containing 150 mM NaBr to remove excess calcium prior to running the gels and assaying for O_2 evolution. Failure to remove calcium resulted in poor quality gels. Table II reports light-induced O_2-evolution rates for the samples in Fig. 8. For comparison, O_2-evolution rates also are shown for $CaCl_2$-treated membranes. With no $CaBr_2$ or $CaCl_2$ in the assay medium, O_2 evolution is minimal in samples treated with 0.6 M or 0.8 M $CaBr_2$. However, addition of 50 mM $CaBr_2$ (or $CaCl_2$, data not shown) to the assay solution greatly increases the rate of O_2 evolution in all $CaBr_2$-treated membranes, but the relative increase (see values in parentheses) was greatest for 0.6 M $CaBr_2$-treated OES II membranes. This titration was the basis for examining 0.6 M $CaBr_2$-treated OES II membranes in subsequent experiments. The results for 50 mM $CaCl_2$ addition to the assay media for $CaCl_2$-treated OES II membranes are as expected (Ref. 33 and Fig. 6). As discussed above, Ono and Inoue [33] used this assay to show that Mn was functional in Ca-treated OES II membranes and that they bind approx. 4 Mn per reaction center. We confirm these results in our $CaCl_2$-treated OES II and by analogy in $CaBr_2$-treated OES II membranes.

Fig. 9 shows SERS spectra of both $CaCl_2$-treated and $CaBr_2$-treated OES II membranes from spinach. Note that the 225 cm^{-1} peak apparent in

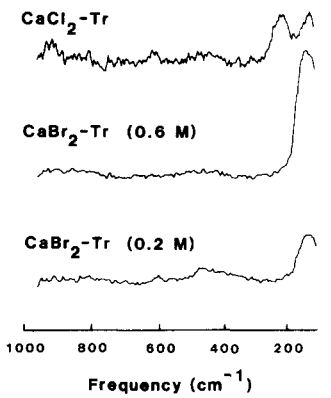

Fig. 9. SERS spectra of $CaCl_2$- and $CaBr_2$-treated OES II membranes from spinach. The 17-, 23- and 33-kDa extrinsic proteins are missing in 0.8 M $CaCl_2$- and 0.6 M $CaBr_2$-treated preparations. The 33-kDa protein remains on the 0.2 M $CaBr_2$-treated OES II preparation. The peak frequencies are 225 and 132 cm^{-1} ($CaCl_2$-treated), 139 cm^{-1} (0.6 M $CaBr_2$-treated), and 145 cm^{-1} (0.2 M $CaBr_2$-treated). Scans, 16.

the chloride-treated membranes is missing in the bromide-treated membranes. Instead a peak at about 140 cm^{-1} is the only feature apparent. The fact that this peak appears at a lower frequency than 225 cm^{-1} is consistent qualitatively with an Mn-ligand vibration in which bromide was substituted for chloride; however, the shift is much greater than would be predicted on simple theoretical grounds (see Discussion). Nevertheless, if part of the 140 cm^{-1} peak in $CaBr_2$-treated membranes is due to a shift of the 225 cm^{-1} peak to lower frequency, then one would expect that the 33-kDa protein would mask part of the 140 cm^{-1} peak in 0.2 M $CaBr_2$-treated membranes. The rationale for this is that the 225 cm^{-1} peak is masked in 2 M $NaCl_2$-treated preparations [20]. These conditions remove the 17- and 23-kDa extrinsic proteins, but not the 33-kDa protein. That the 140 cm^{-1} peak in 0.2 M $CaBr_2$-treated OES II membranes (which contain the 33 kDa protein, Fig. 8) is much smaller than the peak in 0.6 M treated membranes (Fig. 9) is consistent with this prediction. Presumably the 140 cm^{-1} peak in the latter material is composed of background 140 cm^{-1} signal seen in 0.2 M Ca-treated membranes and an additional 140 cm^{-1} component unmasked by the release of the 33-kDa protein.

In our previous publication [20] and Fig. 5, we noted that the 225 cm^{-1} SERS signal in $CaCl_2$-treated OES II membranes from both spinach and *Scenedesmus* is unstable. Moreover, the signal decreases with kinetics similar to that attributed to the loss of $CaCl_2$-reconstituted O_2 evolution capacity and to the release of membrane-bound Mn as discussed earlier. Fig. 10 shows that the 140 cm^{-1} peak in both 0.2 M and 0.6 M $CaBr_2$-treated OES II membranes does not decay over the period of time that the 225 cm^{-1} peak in $CaCl_2$-treated membranes decays (A peaks in Fig. 5). Unexpectedly though, the 140 cm^{-1} peak in the 0.6 M CaBr-treated sample increases. Thus, in contrast to the results with the 225 cm^{-1} SERS peak in $CaCl_2$-treated samples [20], there is not a straightforward relationship between the intensity of 140 cm^{-1} peak in $CaBr_2$-treated samples and the loss of O_2 evolution capacity (and hence the loss of Mn). However, in Fig. 11 we note that there is a relationship between the time-dependent loss of O_2-evolution capacity of 0.6 M $CaBr_2$-

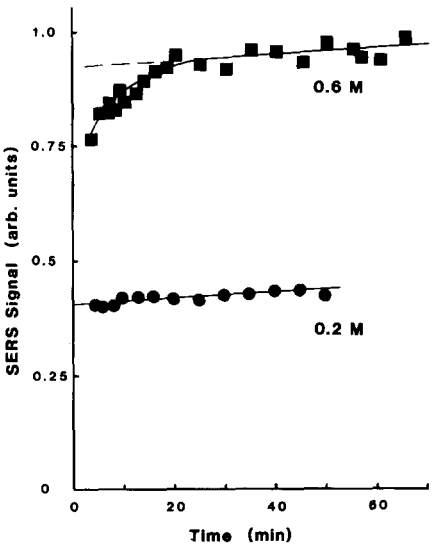

Fig. 10. Time dependence of the 140 cm^{-1} peak intensities of 0.2 M and 0.6 M $CaBr_2$-treated OES II membranes from Fig. 9.

treated OES II membranes and the kinetics of the varying component of the 140 cm^{-1} curve (see Discussion) observed in similar samples (Fig. 10).

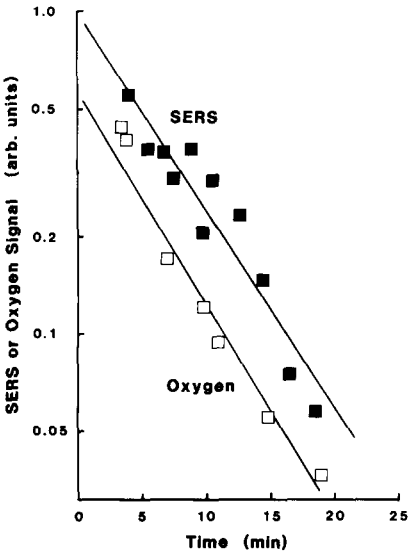

Fig. 11. First-order plot of the 140 cm^{-1} SERS signal from Fig. 10 and the decrease in O_2-evolution rate of 0.6 M $CaBr_2$-treated membranes. For ease of comparison the absolute value of the SERS signal is plotted (the difference between the dashed line and the solid curve in Fig. 10). The O_2 rates were obtained in the presence of 50 mM $CaBr_2$ and 100 mM Na_2SO_4.

Fig. 11 also demonstrates that O_2 evolution capacity in the case of the $CaBr_2$-treated preparations falls off more rapidly than that in $CaCl_2$-treated membranes (see Fig. 3 in Ref. 20).

Discussion

SERS as a probe for Mn

The current study not only confirms the observation of a 225 cm^{-1} SERS signal in $CaCl_2$-treated OES II membranes from spinach that we reported previously [20] but also demonstrates that a similar signal can be seen in green algae (Fig. 4). We have suggested that the signal is related to the presence of functional Mn on the surface of OES II membrane fragments from which the extrinsic proteins associated with O_2 evolution have been removed. Several lines of evidence support this conclusion: the 225 cm^{-1} signal (1) is observed in $CaCl_2$-treated OES II membranes which lack the extrinsic proteins but contain functional Mn (Figs. 3 and 4, Table I, and Ref. 20); (2) is not observed in Tris- and heat-treated OES II membranes which lack both the extrinsic proteins and Mn (Ref. 20, Table I, and Fig. 7); (3) disappears upon aging of $CaCl_2$-treated samples in the SERS cell with kinetics similar to the loss of O_2-evolving capacity and Mn (Ref. 20 and Fig. 6); and (4) is eliminated immediately upon addition of H_2O_2 to $CaCl_2$-treated OES II (Fig. 7). We have shown elsewhere that H_2O_2 removes functional Mn from Ca-treated material upon exposure to light [34].

Furthermore, the signal is not related to Ca used in the treatment of OES II membranes, since $MgCl_2$ treatment also unmasks the same 225 cm^{-1} scattering band (Fig. 3). If a Ca-related vibrational mode were the source of the 225 cm^{-1} signal, the substitution of Mg would shift the signal to higher frequency (because the atomic weight of Mg is less than Ca).

Since the 225 cm^{-1} SERS signal can be related to functional Mn, the question arises whether it is a direct probe of a Mn-ligand vibration or a secondary probe that merely monitors the presence of the functional Mn. If the latter is the case, one would expect that the atoms associated with the vibrational mode that is actually being probed must be released along with the Mn or that a conformational change due to the loss of Mn masks the monitoring vibrational signal. That the vibrational mode is observed at such a low frequency suggests that heavy atoms participate in the chemical bond that is being detected. Besides Mn, Fe is a prime candidate, since it is found in PS II membranes. Furthermore, Fe and Mn differ by only one atomic weight unit so that Fe- and Mn-ligand vibrations should be very similar. Table I shows that Fe is not released from the membrane under conditions that release Mn and lead to the disappearance of the 225 cm^{-1} SERS signal. Thus, we rule out an Fe-ligand vibration as the origin of the SERS signal. In the absence of any evidence for other candidate metals in the neighborhood of Mn or masking conformational changes, we shall consider the possibility that we are detecting a Mn-ligand vibrational mode directly. Possible ligands are Cl, N, and O. This is not at all unreasonable, since synthetic Mn complexes have absorption peaks at about 500 nm (Ref. 39, see also Sheets, J.E., personal communication), close to the excitation wavelength used in these experiments. Moreover, low-frequency Mn-ligand vibrations have been reported in the vicinity of 225 cm^{-1} [40,41] although higher frequencies also are reported. Thus, it is possible that we may be seeing a resonance-enhanced, in addition to a surface-enhanced, signal (i.e., a SERRS signal).

Relationship to Cl

It has been postulated that Cl serves as a ligand to Mn [42] and that it stabilizes higher oxidation states of the metal [43]. However, it also has been suggested that Cl might facilitate electron transfer by binding near the active site of the OEC [44] where it would stabilize the conformation necessary for water oxidation through a charge neutralization mechanism [45]. Recent EXAFS studies of OES II preparations provide no evidence for a Cl ligand in the first coordination sphere of Mn although the work cannot rule out the presence of one Cl scatterer per 4 Mn [46]. Nevertheless, the fine structure of the EPR multiline signal does not change when Br is substituted for Cl in OES II preparations suggesting that halide is not involved in the first coordination sphere of the EPR-active Mn in S_2 [47]. Our $CaBr_2$ experiments are consistent with these latter observations. The SERS

spectra of Fig. 9 show that the substitution of bromide for chloride in Ca-treated OES II membranes shifts the 225 cm^{-1} SERS signal to 140 cm^{-1}. Since the frequency of a Raman scattering peak is inversely related to the square root of the combined atomic weight of the species (Mn and Cl or Br in our case) forming the chemical bond being probed, the expected peak shift should be to about 184 cm^{-1}. Thus, the shift to 140 cm^{-1} that we observe is too great to be explained by Cl located in the first coordination sphere of Mn.

The 33-kDa protein covers Mn

In our previous study [20], we showed that the 33-kDa protein covers the source of the 225 cm^{-1} SERS signal and hence Mn because the signal could not be seen in OES II membranes that bind the 33-kDa protein. (These membranes lacked the 17- and 23-kDa proteins, whereas the control membranes in Fig. 3 bind all three extrinsic proteins.) Although the situation with $CaBr_2$-treated OES II is more complex, the same conclusion can be inferred. There is substantial background scattering at 140 cm^{-1} (see Figs. 3, 4 and 9 in control, $CaCl_2$- and $CaBr_2$-treated OES II membranes) probably due to Ag_4^+ clusters on the electrode surface [30]. However, the 140 cm^{-1} signal increases in $CaBr_2$-treated OES II when the 33-kDa protein is released (see Figs. 8 and 9). This increase in signal is not related to the increased amount of $CaBr_2$ necessary to release the 33-kDa protein, since excess $CaBr_2$ is removed from the membranes by several washing steps (see Materials and Methods). Furthermore, part of the 140 cm^{-1} signal varies with time in membranes lacking the 33-kDa protein (0.6 M $CaBr_2$ in Fig. 10), whereas the 140 cm^{-1} background signal is stable when the 33-kDa protein is bound to the membrane (0.2 M $CaBr_2$ in Fig. 10). In $CaCl_2$-treated OES II, the 225 cm^{-1} signal was unstable. Moreover, the loss of signal upon aging could be related kinetically to the loss of O_2-evolution capacity and hence the loss of Mn present on the membrane (Ref. 20 and Fig. 6). We can also relate the unstable component of the 140 cm^{-1} peak in 0.6 M $CaBr_2$-treated OES II kinetically to the loss of O_2-evolution capacity. However, in this case the SERS signal increases (see Figs. 10 and 11) instead of decreasing. For ease of comparison with the O_2 data, we have plotted the absolute value of the variable component of the 140 cm^{-1} signal in Fig. 11. The reason for the increase is not known. However, one might speculate that upon aging of 0.6 M $CaBr_2$-treated membranes, bromide is released from the membranes along with Mn. SERS signals due to Ag-Br-water surface complexes are well known and are commonly observed at 110–170 cm^{-1} [32]. If Br destabilized from the membranes interacts with the Ag SERS-active electrode, Ag-Br complexes might form on the electrode surface. A greater scattering intensity of Ag-Br complexes on the electrode surface than scattering observed when Mn and Br are bound to the membrane could explain the 'growing in' effect.

Relationship of Mn to the D1 protein

$CaCl_2$-treated PS II membranes from the LF-1 mutant of *Scenedesmus* contain about half the Mn of similar membranes from WT (Table I). Since the mutant is affected in the D1 protein [36] and the dark decay kinetics of the 225 cm^{-1} peak in LF-1 is much faster than in the WT (Fig. 5), we suggest that the normal SERS signal in WT is related to Mn bound to the D1 protein. Furthermore, we suggest that the 33-kDa protein covers that site as discussed in the previous section.

The source of the 225 cm^{-1} SERS signal

This study provides ample evidence that the 225 cm^{-1} SERS signal is related to the presence of functional Mn on the surface of OES II membranes lacking the extrinsic proteins. However, it is probably not due to scattering by an Mn-Cl vibrational mode and may even be an indirect probe dependent on the presence of Mn and halide on the membrane. Other possible sources of the signal that remain to be examined include: (1) an Mn-O or Mn-N vibrational mode modified by chloride not present in the first coordination sphere; (2) a cooperative effect associated with the protein environment around the Mn-binding site that changes with the presence of halide; and (3) a species associated primarily with the Ag electrode that changes depending on the presence or absence of Mn and halide on the surface of the membrane. This last possibility might explain the curious increase in scattering at 140 cm^{-1} ob-

served in 0.6 M $CaBr_2$-treated OES II (Fig. 10) and the rapidly disappearing 225 cm^{-1} signal in $CaCl_2$-treated PS II membranes of *Scenedesmus* LF-1 (Fig. 5).

Acknowledgements

This work was supported by a Chemistry of Life Processes grant (No. CHE-8509594), from NSF, to T.M.C. and M.S. Some preliminary work that lead to this study was sponsored by the Divisions of Biological Energy Research (FTP 006-85; M.S.) and Chemical Sciences (DE-F602-84-ER13261; T.M.C.), Office of Basic Energy Sciences, U.S. Department of Energy. The authors would like to thank D. Cohen for expert assistance in preparing the spinach OES II membranes and running the gel, Drs. T. Furtak and V.K. Yachandra for sharing their unpublished manuscripts with us, and Dr. J. Bolton for stimulating discussions of this work.

References

1 Otto, A. (1984) in Light Scattering in Solids IV (Cardona, M. and Güntherodt, G., eds.), pp. 289–418, Springer-Verlag, New York.
2 Fleischmann, M., Hendra, P.F. and McQuillan, A.J. (1974) Chem. Phys. Lett. 26, 123.
3 Jeanmaire, D.L. and Van Duyne, R.P. (1977) J. Electroanal. Chem. 84, 1–20.
4 Albrecht, M.G. and Creighton, J.A. (1977) J. Am. Chem. Soc. 99, 5215–5217.
5 Chang, R.K. and Laube, B.L. (1984) CRC Crit. Rev. in Solid State Mat. Sci. 82, 1–73.
6 Blatchford, C.G., Campbell, J.R. and Creighton, J.A. (1982) Surf. Sci. 120, 435–455.
7 Metiu, H. (1982) in Surface Enhanced Raman Scattering (Chang, R.K. and Furtak, T.E., eds.), pp. 1–34, Plenum Press, New York.
8 Seki, H. (1983) J. Electron Spec. Related Phen. 30, 287.
9 Nabiev, I.R., Savchenko, V.A. and Efrencov, E.S. (1983) J. Raman. Spec. 14, 375–379.
10 Ervin, K.M., Koglin, E., Sequaris, J.M., Valenta, P. and Nürnberg, H. W. (1980) J. Electroanal. Chem. 114, 179–194.
11 Sequaris, J.-M., Koglin, E., Valenta, P. and Nürnberg, H.W. (1981) Ber. Bunsenges. Phys. Chem. 85, 512–513.
12 Koglin, E., Sequaris, J.M. and Valenta, P.Z. (1981) Naturforsch. 36C, 809–812.
13 Sequaris, J.M., Koglin, E. and Malfoy, B. (1984) FEBS Lett. 173, 95–98.
14 Knoll, W., Philpott, M.R. and Golden, W.G. (1982) J. Chem. Phys. 77, 219–225.
15 Cotton, T.M., Schultz, S.G. and Van Duyne, R.P. (1980) J. Am. Chem. Soc. 102, 7960–7962.
16 Cotton, T.M., Timkovich, R. and Cork, M.S. (1981) FEBS Lett. 133, 39–44.
17 Cotton, T.M. and Holt, R. (1987) J. Am. Chem. Soc. 109, 1841–1845.
18 Copeland, R.A., Fodor, S.P.A. and Spiro, T.F. (1984) J. Am. Chem. Soc. 106, 3872–3874.
19 Cotton, T.M. and Van Duyne, R.P. (1982) FEBS Lett. 147, 81–84.
20 Seibert, M. and Cotton, T. (1985) FEBS Lett. 182, 34–38.
21 Picorel, R., Holt, R.E., Cotton, T.M. and Seibert, M. (1988) J. Biol. Chem., 263, 4374–4380.
22 Dunahay, T.G., Staehelin, L.A., Seibert, M., Ogilvie, P.D. and Berg, S.P. (1984) Biochim. Biophys. Acta 764, 179–193.
23 Ono, T.-A. and Inoue, Y. (1983) FEBS Lett. 164, 255–260.
24 Ogilvie, P.D., Reschl, L.B. and Berg, S.P. (1983) Arch. Biochem. Biophys. 220, 451–458.
25 Ikeuchi, M., Yuasa, M. and Inoue, Y. (1985) FEBS Lett. 185, 316–322.
26 Metz, J.G. and Seibert, M. (1984) Plant Physiol. 76, 829–832.
27 Metz, J. and Bishop, N.I. (1980) Biochem. Biophys. Res. Commun. 94, 560–566.
28 Jeanmaire, D.L., Sushanski, M.S. and Van Duyne, R.P. (1985) J. Am. Chem. Soc. 97, 1699–1706.
29 Seibert, M., DeWit, M. and Staehelin, L.A. (1987) J. Cell Biol. 105, 2257–2265.
30 Roy, D. and Furtak, T.E. (1986) Phys. Rev. B 34, 5111–5117.
31 Fleischmann, M., Hill, I.R. and Sundholm, G. (1983) J. Electroanal. Chem. 158, 153–164.
32 Rogers, D.J., Luck, S.D., Irish, D.E., Guzonas, D.A. and Atkinson, G.F. (1984) J. Electroanal. Chem. 167, 237–249.
33 Ono, T.-A. and Inoue, Y. (1984) FEBS Lett. 168, 281–286.
34 Berg, S.P. and Seibert, M. (1987) Photosynth. Res. 13, 3–17.
35 Kitagawa, T., Nagai, K. and Tsubaki, M. (1979) FEBS Lett. 104, 376–378.
36 Metz, J.G., Pakrasi, H.B., Seibert, M. and Arntzen, C.J. (1986) FEBS Lett. 205, 269–274.
37 Nanba, O. and Satoh, K. (1987) Proc. Natl. Acad. Sci. USA 84, 109–112.
38 Seibert, M., Picorel, R., Rubin, A.B. and Connolly, J.S. (1988) Plant Physiol., in press.
39 Nair, B.U. and Dismukes, G.C. (1983) J. Am. Chem. Soc. 105, 124–125.
40 Nakamoto, K. (1978) Infrared and Raman Spectra of Inorganic and Coordinated Compounds, John Wiley & Sons, N.Y., and references cited therein.
41 Asher, S. and Sauer, K. (1976) J. Chem. Phys. 64, 4115–4125.
42 Sandusky, P.O. and Yocum, C.F. (1984) Biochim. Biophys. Acta 766, 603–611.
43 Wydrzynski, T. and Sauer, K. (1980) Biochim. Biophys. Acta 589, 56–70.
44 Critchley, C., Baianu, I.C., Govindjee and Gutowsky, H.S. (1982) Biochim. Biophys. Acta 682, 436–445.
45 Johnson, H.D., Pfister, V.R. and Homann, P. (1983) Biochim. Biophys. Acta 723, 256–265.
46 Yachandra, V.K., Guiles, R.D., McDermott, A.E., Cole, J.L., Britt, R.D., Dexheimer, S.L., Sauer, K. and Klein, M.P. (1987) Biochemistry 26, 5974–5981.
47 Yachandra, V.K., Guiles, R.D., Sauer, K. and Klein, M.P. (1986) Biochim. Biophys. Acta 850, 333–342.